# An *Ab Initio* Study of $CuGaSe_2$ (001) Surface

S. C. Chew[a], L. M. Liborio[a] and N. M. Harrison[a,b]

[a]Thomas Young Centre, Department of Chemistry,
Imperial College London, Exhibition Road, London, SW7 2AZ, United Kingdom
[b]Computational Science and Engineering Department, STFC Daresbury Laboratory,
Daresbury, Warrington, Cheshire, WA4 4AD, United Kingdom
su.chew09@imperial.ac.uk, l.liborio@imperial.ac.uk, nicholas.harrison@imperial.ac.uk

## ABSTRACT

Hybrid density functional calculations have been used to study the atomic and electronic structure of three proposed models for the (4×1) surface reconstruction in the chalcopyrite $CuGaSe_2$ (001) surface. The proposed surface models have been created through Se vacancies, Cu vacancies and Ga substituting Cu type of defects. This structural richness increases the possibility for engineering the $CuGaSe_2$/CdS heterogeneous interface by surface control during growth.

***Keywords***: $CuGaSe_2$, chalcopyrite, solar energy, surface reconstruction, thin films

## 1 INTRODUCTION

The chalcopyrite material makes one of the best performing devices for heterogeneous polycrystalline thin film solar cells. Specifically, the In-rich $Cu(In,Ga)Se_2$ solar cell has reached efficiencies of approximately 19% [1]. Despite this, many of the fundamental properties of this material remain unexplained. In principle, theoretical efficiencies of $CuGaSe_2$ solar cells should be close to those of $Cu(In,Ga)Se_2$. However, current efficiencies in $CuGaSe_2$ solar cells are of the order of 9.5% [2]. More research is needed to employ this material in photovoltaic applications.

A heterojunction solar cell is a multilayered structure, with the top layer being a wide band gap, highly transparent material that acts as a window layer. It allows most of the incident light through to the bottom active layer, which is an n-type material called the buffer layer. The next layer is the absorber layer, which in this case would be made of $CuGaSe_2$ that is p-type material. When light is absorbed into $CuGaSe_2$, electrons from the valence band are excited into the conduction band and electron-hole pairs are created. In an efficient solar cell, these pairs split apart with minimum recombination, and migrate to the cell's electrodes, generating the charge carriers that give rise to the photocurrent. Effective charge separation will critically depend on the physical and chemical structure of the p-n heterojunction formed by the buffer and absorber layer. Therefore, it is important to determine the atomic structure of the $CuGaSe_2$ surface forming the p-n heterojunction.

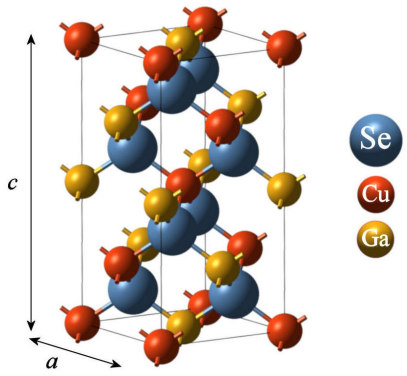


Figure 1: Crystallographic Cell of $CuGaSe_2$

Experiments such as low energy electron diffraction (LEED), Auger electron spectroscopy (AES) and X-ray photoelectron spectroscopy (XPS) have shown that the (001) surface of $CuGaSe_2$ has a clear (4×1) reconstruction, and that it has Cu-poor and Se-rich surface stoichiometry [3], [4]. This study will use *ab initio* calculations to investigate the atomic and electronic structure of the $CuGaSe_2$ (001) surface.

## 2 METHODOLOGY

Density Functional Theory (DFT) calculations were performed using CRYSTAL [5] and the B3LYP hybrid exchange functional [6]. This functional has been shown to provide a reliable description of the electronic structure, geometry and energetics in a wide range of materials [7], [8]. In particular, hybrid exchange functionals such as B3LYP provide a much better prediction of the band gap of semiconductors than LDA or GGA DFT functionals, and are therefore likely to be more accurate in estimating the valence band offset of semiconductor heterojunctions [7].

Polarised triple valence Gaussian basis sets, which have been used in previous studies [8], [9], were used throughout. In the case of Ga, a pseudopotential was used to describe the core electrons [9]. In CRYSTAL, real space summations of the Coulomb and exchange contributions to the Hamiltonian matrix are controlled by five overlap criteria. The values used in the study were $10^{-6}$, $10^{-6}$, $10^{-6}$, $10^{-6}$ and $10^{-12}$. The control of these approximations is described in detail elsewhere

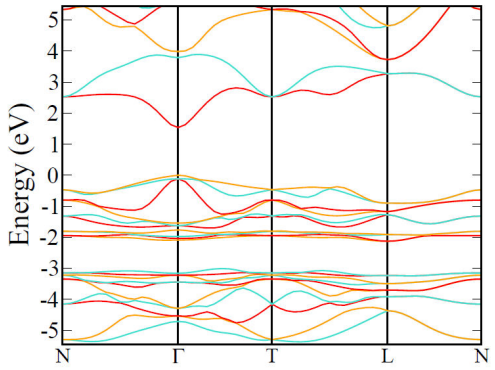


Figure 2: Band Structure of $CuGaSe_2$

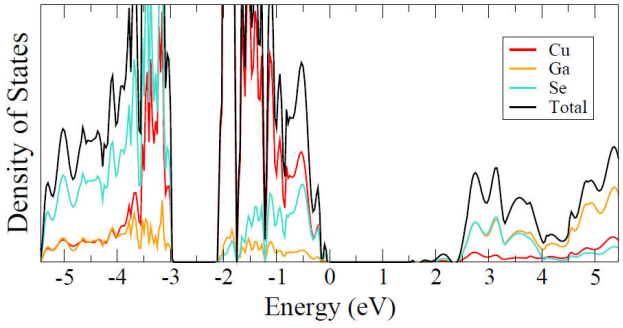


Figure 3: Density of States of $CuGaSe_2$

[5]. A Monkhorst-Pack shrinking factor of 8 was used to sample the first Brillouin zone, and a Gilat net of 8 points was used in the evaluation of the Fermi energy and density matrix [5].

## 3 BULK PROPERTIES

The crystallographic cell of the $CuGaSe_2$ is shown in Figure 1, and has a body centered tetragonal lattice, with the c axis normal to the (001) surface. It is often described as a double zinc blende unit cell, with Cu and Ga atoms replacing the Zn atom, and Se atom replacing the S atom. The presence of two different cations give it a wider range of physical and chemical properties compared to binary semiconductors.

The relaxed lattice parameters of bulk $CuGaSe_2$ are calculated to be $a = 5.739$ Å and $c = 11.311$ Å, versus experimental values of 5.614 Å and 11.022 Å [10]. The reduced symmetry due to the tetragonal distortion of the unit cell is described by $\eta = c/2a$, which is 0.985 and compares well with the experimental value of 0.982.

A direct band gap of 1.537 eV is calculated, which is in good agreement of the experimental value of 1.68 eV [11]. The band structure is shown in Figure 2 and the points chosen for the Brillouin Zone path are Γ(0,0,0), N($\pi$/a,$\pi$/a,0), T(0,0,$\pi$/a) and L ($\pi$/a,$\pi$/a,$\pi$/a).

The calculated density of states (DOS) of $CuGaSe_2$ is shown in Figure 3. Cu contributes most to the DOS at the top of the valence band, followed closely by Se. Se and Ga contribute the most DOS to the bottom of the conduction band.

## 4 SURFACE RECONSTRUCTIONS

### 4.1 Models of the (4×1) reconstruction

The $CuGaSe_2$ consists of alternating layers of Se and CuGa atoms in the (001) direction. The same termination is kept for both top and bottom surfaces of the slabs, and thus the modelled slab is non-stoichiometric. We begin our calculations with a Se-terminated slab, which is converged to a precision of 21 meV/$a^2$ at 17 layers, and has starting Se-rich stoichiometry of $CuGaSe_{2.25}$. In this paper we discuss three of types of surface reconstructions created by Se vacancies ($V_{Se}$), Cu vacancies ($V_{Cu}$) and Ga-on-Cu antisite ($Ga_{Cu}$), and are shown in Figure 4.

Figure 4A shows the top and lateral view of the unreconstructed Se-terminated surface. The (4×1) surface unit cell is indicated by a black rectangle. Atomic positions of Se in the top layer of the surface unit cell are labelled 1 to 8.

Figure 4B shows a reconstruction made by creating two distant $V_{Se}$ at Se positions 2 and 5. This exposes the CuGa layer beneath and one of the Cu beneath the $V_{Se}$ at position 2 is removed to create a Cu-poor stoichiometry (Reconstruction B).

Reconstruction C is made by removing half of Se from the surface. The four $V_{Se}$ are created at positions 2, 4, 5 and 7, making a (2×1) reconstruction. The Se at nearby positions 2 and 7 were attached to the same Cu in the layer below. Removal of a single Cu beneath $V_{Se}$ at position 2 and 7 reduces the periodicity of the surface to (4×1).

Reconstruction D is made by introducing two $V_{Se}$ at nearby positions 3 and 8, and were attached to the same Cu below. This Cu is substituted with Ga.

### 4.2 Electron charge density

One of the ways to help elucidate the nature of reconstructions at the surface experimentally is by scanning tunneling microscopy (STM). The resolution of the STM is a result of the quantum mechanical tunnelling between the microscope's tip and the studied sample. To first order, the tunnelling current itself is a function of tip position, applied voltage, and the local density of states (LDOS) of the sample's surface [12]. Using *ab initio* calculations it is possible to calculate the spatially resolved electronic DOS at the different $CuGaSe_2$ (001) (4×1) surface reconstructions. Therefore, such data can be useful in the intepretation and prediction of the experimental STM images.

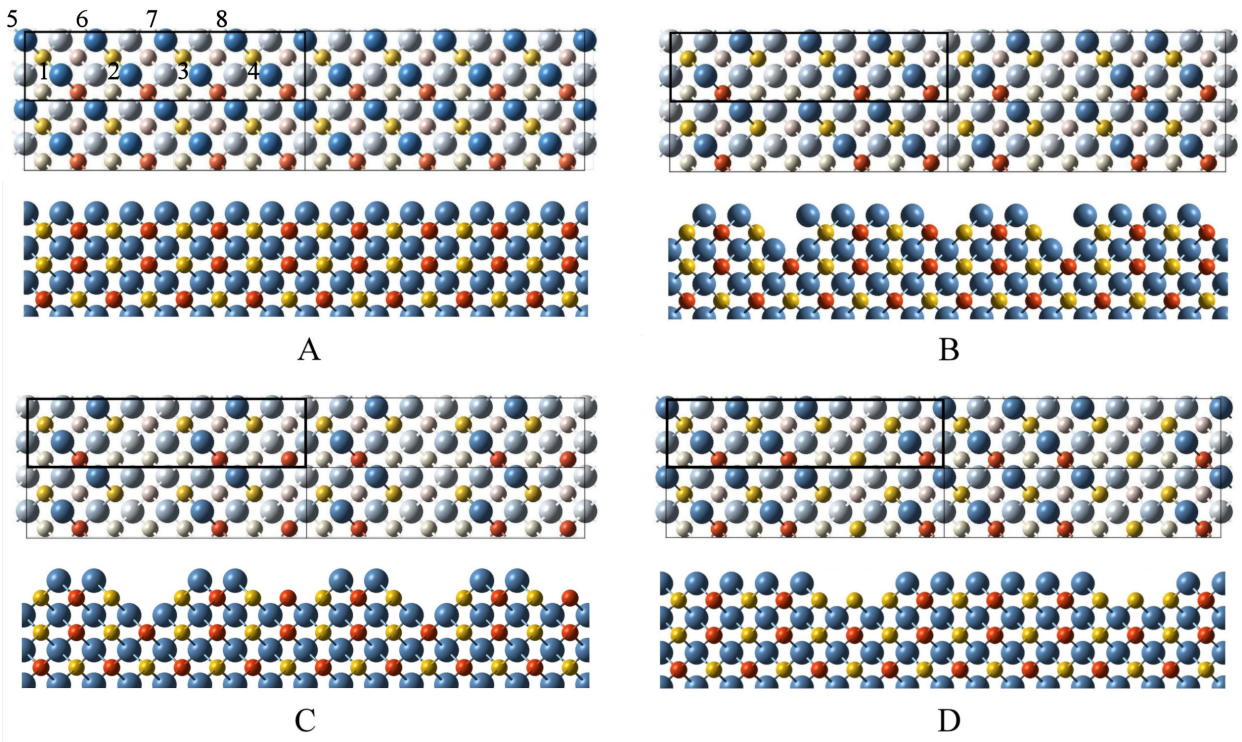


Figure 4: Top and lateral views of possible (4×1) surface reconstructions. A: Unreconstructured Se-terminated surface. B: $2V_{Se}$ at positions 2 and 5, and $V_{Cu}$ beneath $V_{Se}$ at position 2. C: $4V_{Se}$ at positions 2, 4, 5 and 7, and $V_{Cu}$ beneath $V_{Se}$ at 2 and 7. D: $2V_{Se}$ at positions 3 and 8, and $Ga_{Cu}$ beneath.

In Figure 5 the top pictures on each quadrant show the electron charge density map for the top view of the surface reconstruction. The upper left quadrant shows the electron charge density map at the first layer of the slab, and the upper right quadrant for the second layer of the slab. The electron charge density map for the lateral view of the surface reconstructions are in shown in the bottom quadrants. The bottom left quadrant shows the electron charge density map when the plane is cut perpendicular to the (001) surface along the Se at M-N, whereas the bottom right quadrant shows the electron charge density map when the plane is cut perpendicular to the (001) surface along the Cu at O-P. This is illustrated in Figure 5A.

Figures 5B and 5C in the bottom left quadrant indicates that the outermost electronic density isolines have a significant depression above the Cu vacancies region. Since the STM spots brightness is modulated by the tip's vertical position, the depressions would be correlated with a change in the image's brightness in a constant current STM image. In the top quadrants of Figures 5B and 5C, the region above the Cu vacancies shows no electronic density. The combination of top and lateral views indicates that the STM image of these reconstructions is likely to have bright lines separated by a distance of $4a$. The STM images of Reconstruction D will be equivalent, but in this case the bright lines will be related with depressions at the Se vacancies positions.

## 5 CONCLUSION

*Ab initio* calculations were performed using B3LYP hybrid exchange functional for the bulk and (001) surfaces of $CuGaSe_2$. Lattice parameters of the relaxed bulk were calculated to be $a = 5.739$ Å and $c = 11.311$ Å. A direct band gap of 1.537 eV is given, and a DOS calculation shows that the DOS at the top of the valence band is contributed mostly by Cu and Se. Se and Ga are the major contributers to the DOS at the bottom of the conduction band.

We have calculated the spatially resolved electronic density for different $CuGaSe_2$ (001) (4×1) surface reconstructions, and the results can be used to estimate experimental STM images.

The relative stabilities of the surface reconstructions will depend on the growth conditions and preparation of the sample. Thus we must determine the surface energies of the various surface reconstructions as a function of the growing conditions. This will be done by using the formalism known as *ab initio* thermodynamics, which combines results from DFT with concepts from classical thermodynamics. Such methods can help in the engineering the $CuGaSe_2$/CdS heterogeneous inter-

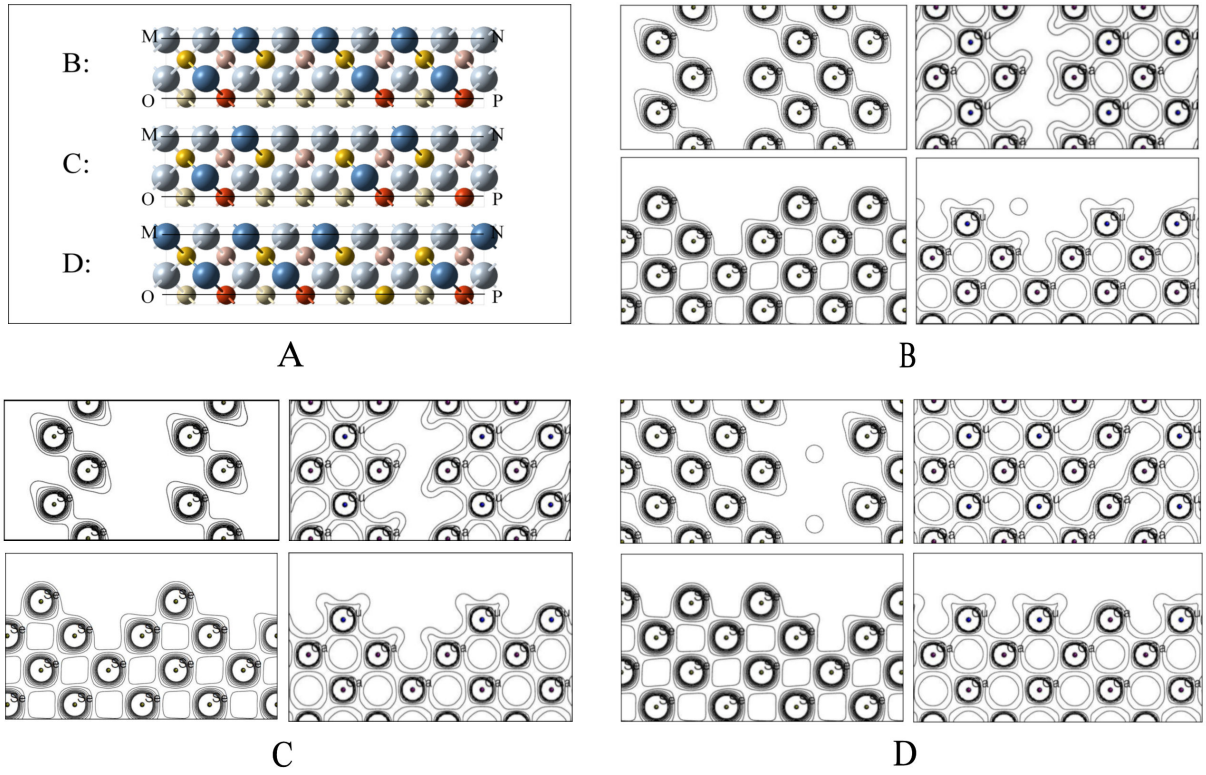


Figure 5: Isolines of constant electronic density in planes representing top and lateral views of surface reconstructions B, C and D. The isolines in the figures represent absolute values of the electronic of the density in atomic units (electron/bohr$^3$) and span the range from 0.01 to 0.1 a.u with a step of 0.01 a.u.

face, and have been used before in the investigation of the (112) and ($\overline{112}$) chalcopyrite $CuInSe_2$ material [13].

## REFERENCES


[1] Green MA, Emery K, Hishikawa Y, Warta W. Solar cell efficiency tables (Version 35). Prog Photovolt Res Appl. 2010;18(2):144 – 150.

[2] Siebentritt S. Wide gap chalcopyrites: material properties and solar cells. Thin Solid Films. 2002;403-404:1 – 8. Proceedings of Symposium P on Thin Film Materials for Photovoltaics.

[3] Deniozou T, Esser N, Siebentritt S, Vogt P, Hunger R. Surface structure of $CuGaSe_2$ (001). Thin Solid Films. 2005;480-481:382 – 387.

[4] Deniozou T, Esser N, Siebentritt S. The $CuGaSe_2$ (001) surface: A (41) reconstruction. Surf Sci. 2005;579(1):100 – 106.

[5] Dovesi R, Saunders VR, Roetti C, Orlando R, Zicovich-Wilson CM, Pascale F, et al. CRYSTAL 2006 Users's Manual. University of Torino; 2007.

[6] Becke AD. A new mixing of Hartree-Fock and local density-functional theories. J Chem Phys. 1993;98:1372.

[7] Muscat J, Wander A, Harrison NM. On the prediction of band gaps from hybrid functional theory. Chem Phys Letts. 2001;342:397.

[8] Tomić S, Montanari B, Harrison NM. The group III-V's semiconductor energy gaps predicted using the B3LYP hybrid functional. Physica E. 2008;40:2125.

[9] Heyd J, Peralta JE, Scuseria GE, Martin RL. Energy band gaps and lattice parameters evaluated with the Heyd-Scuseria-Ernzerhof screened hybrid functional. J Chem Phys. 2005;123:174101.

[10] Mandel L, Tomlinson RD, Hampshire MJ. Crystal data for $CuGaSe_2$. J Appl Crystallogr. 1977 Apr;10(2):130 – 131.

[11] Shay JL, Tell B, Kasper HM, Schiavone LM. $p-d$ Hybridization of the Valence Bands of I-III-$VI_2$ Compounds. Phys Rev B. 1972 Jun;5(12):5003–5005.

[12] Tersoff J, Hamann DR. Theory of the scanning tunneling microscope. Phys Rev B. 1985 Jan;31(2):805–813.

[13] Zhang SB, Wei SH. Reconstruction and energetics of the polar (112) and ($\overline{112}$) versus the nonpolar (220) surfaces of $CuInSe_2$. Phys Rev B. 2002 Feb;65(8):081402.